to the authors by Dr. Khare.

[39]R. W. LaBahn and J. Callaway, Phys. Rev. 180, 91 (1969).

[40]J. P. Bromberg, J. Chem. Phys. 50, 3906 (1969).

[41]J. Callaway, R. W. LaBahn, R. T. Pu, and W. M. Duxler, Phys. Rev. 168, 12 (1968).

[42]The renormalization was carried out by setting $\alpha^2 = 3.39$ in Eq. (3) and adjusting f_0 to give agreement with the absolute measurements at 5°. This procedure assumes an angular shape for angles that have not been measured, particularly for the important region of 0° to 5° over which, at 400 eV, the differential cross section makes more than a 50% contribution to the total cross section. Recent experimental measurements [E. N. Lassettre, A. Skerbele, and M. A. Dillon, J. Chem. Phys. 50, 1829 (1969)] over the angular range 2.5°–6° (at 500 eV) show a cross section dependence on K^2 that decreases less rapidly, for small K^2 (0.08 to 0.41), than the angular dependence we assumed. We estimate that the change in the total cross section at 400 eV would be less than 3% if we used the cross-section dependence on small momentum transfer given by Lassettre *et al.*

[43]J. van Eck and J. P. de Jong, Physica 47, 141 (1970).

[44]K. L. Bell, D. J. Kennedy, and A. E. Kingston, J. Phys. B 2, 26 (1969).

[45]J. D. Jobe and R. M. St. John, Phys. Rev. 164, 117 (1967).

[46]J. D. Jobe (private communication).

PHYSICAL REVIEW A VOLUME 2, NUMBER 5 NOVEMBER 1970

Alkali-Alkali Differential Spin-Exchange Scattering. I*

David E. Pritchard, Gary M. Carter†, Frank Y. Chu, and Daniel Kleppner
Physics Department and Research Laboratory for Electronics, Massachusetts Institute of Technology, Cambridge, Massachusetts 02139

(Received 7 April 1970)

We present measurements of differential elastic cross sections for various alkali-alkali pairs, as well as the angular dependence of the probability of electron spin exchange in these collisions. The resolution is sufficient to reveal interference structure in the angular dependence of both quantities. We describe our apparatus, which polarizes one incident beam and analyzes the polarization of the scattered atoms, and discuss the measurement and data-reduction procedures. Results are presented in the range 0.1–0.2 eV for the systems Na-Cs, Na-Rb, Na-K, K-Cs, and K-Rb.

I. INTRODUCTION

Much of our present knowledge of interatomic and intermolecular interactions comes from atomic- and molecular-beam scattering studies. During recent years there has been a steady progression in atomic scattering technique, with a corresponding elaboration of the details of interaction. In the thermal energy range this has been due primarily to increased resolution of velocity and angle. Measurements of the elastic differential cross section now yield very accurate potential curves for systems characterized by a single potential; Pauly's work on alkali–rare-gas systems is a notable example.[1] In more complicated systems there are additional degrees of freedom which govern the interaction. Such systems cannot be adequately described by a single potential, and in order to investigate them experimentally, the scattering apparatus must be able to resolve all the available degrees of freedom.

This paper reports a step in this direction by describing experiments on alkali-alkali interactions which depend on the total spin of the two valence electrons. There are two interaction potentials depending on whether the total spin is 1 or 0, corresponding to the triplet and the singlet state, respectively. Due to the exclusion principle, the singlet interaction is more attractive than the triplet interaction, and the singlet potential lies below the triplet potential at moderate internuclear separations ($5-20\,a_0$). This effect is the result of symmetry, not of direct coupling between the spins. (Direct spin-spin coupling of the valence electrons is sufficiently small to be neglected during the collision.)

The measurements of spin-dependent differential cross sections presented here provide a sensitive measure of the singlet and triplet potentials involved. In experiments without spin-resolution the observed differential cross section [which we call $\sigma_{\text{sum}}(\theta)$] is a weighted average of the cross sections which would be produced by the potentials acting separately. In the present experiments the electron spin of one of the atoms is polarized before the collision and analyzed afterwards, enabling us to measure the probability that scattering through a given angle will be accompanied by exchange of the electron spin, $P_{\text{ex}}(\theta)$. The spin-exchange process results from interference between the singlet and triplet scattering amplitudes and therefore provides a key for separately determining the potentials.

The significance of spin exchange was first ap-

preciated by Purcell and Field,[2] who studied the role of spin exchange in establishing the spin temperature in interstellar hydrogen, and by Wittke and Dicke,[3] who analyzed the role of spin exchange on relaxation of radiating hydrogen atoms. Dehmelt[4] suggested the use of spin exchange as a mechanism for transferring and analyzing polarization in optical pumping experiments. It has since been widely used in this connection and many observations have been made of total spin-exchange cross sections by optical pumping techniques.[5] However, these are all concerned with total cross sections averaged over a broad energy distribution.

Recently there have been several measurements of differential spin-exchange scattering. In the case of alkali-alkali scattering, preliminary results of the present work[6] and results by Beck and his colleagues[7] have already appeared. Bederson and his co-workers[8] have obtained differential spin-exchange cross sections for electron-alkali collisions. In contrast to earlier measurements of the total spin-exchange cross section by optical pumping techniques, these new measurements permit determination of details in the relevant interatomic potentials which are beyond the range of current theoretical predictions of these potentials. We hope that these results will stimulate the development and application of techniques for calculating these potentials.

This is the first in a series of three papers on spin-exchange collisions between alkali atoms. In this paper we describe the apparatus and present experimental results; in Paper II, we discuss a theoretical framework which connects the features of the potentials with the observations. We will present a more complete analysis of the potentials for various nonidentical alkali-alkali systems in a later publication.

In this paper we describe our spin-exchange scattering apparatus and experimental procedure. We present results of $\sigma_{sum}(\theta)$ and $P_{ex}(\theta)$ for the following nonidentical pairs of alkali atoms: Na-K, Na-Rb, Na-Cs, K-Rb, and K-Cs.

II. APPARATUS

These spin-exchange measurements were made in a crossed atomic-beam scattering apparatus in which a spin-selected primary beam collides with an unpolarized crossed beam.[9] The spin state of the scattered beam is analyzed to determine the differential cross section for scattering into each of the possible final spin states.

The apparatus is shown schematically in Fig. 1. The source of atoms is an alkali oven which is generally operated in the region of supersonic flow. A hot skimmer restricts the width of the emerging beam. The atoms are state selected by an inhomogeneous magnetic field; either spin state can be selected by changing the position of the oven relative to the magnet by means of an electric drive mechanism. The beam passes through a collimator into the scattering region where it collides with a modulated target beam. Atoms scattered through the exit slit toward the detector are velocity analyzed by a slotted-disk velocity selector and then pass through a second magnetic state selector which separates them into two beams according to spin. The emerging beams are detected separately by two hot-wire detectors. Operating characteristics of the apparatus are summarized in Table I. Further details follow.

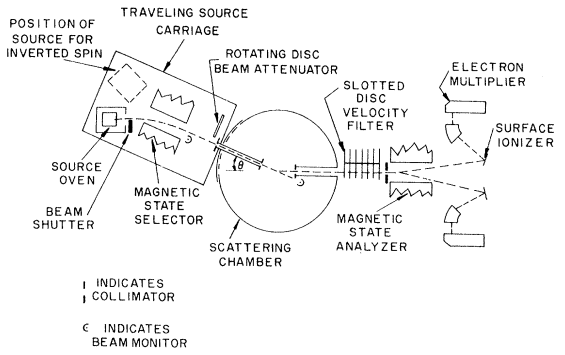

FIG. 1. Schematic view of apparatus. Neither of the two different target-beam sources is shown.

A. State Selectors

Both state selectors are of the familiar two-wire field configuration.[10] The incident-beam state selector is a permanent magnet while the scattered-beam state selector is an electromagnet whose coils are mounted outside of the vacuum system. Iron inserts conduct the flux through the stainless-steel vacuum envelope. Operating characteristics of the magnets are given in Table I.

B. Beam Attenuator

During the initial alignment process and during checks of the polarization of the incident beam, the detector must be exposed to the primary beam. Because even short exposure to the full primary flux causes prohibitive background in the detector, a beam attenuator is used to reduce the flux. This consists of a rotating disc with a series of holes which intersects the beam; either four holes 0.75 mm diam on a 7-cm-diam circle, or one hole 0.075 mm diam on a 6.35-cm-diam circle. These give attenuation factors of ~700 and $\sim 3\times10^5$, respectively. In order to investigate the shape of the beam the attenuator can be swept across the beam by a drive mechanism which also inserts and removes it.

C. Sources

The primary beam is produced by a conventional

TABLE I. Operating Characteristics.

Polarized primary-beam intensity	0.3×10^{12}	atoms/sec
Target-beam density	1×10^{12}	atoms/cm^3
Angular resolution	2×10^{-3} rad	full width
Velocity resolution	5% or 10%	FWHM
Beam dimensions		
Primary beam	0.2 mm×5 mm	width×height
Scattered beam	0.4 mm×5 mm	width×height
Target beam	2.5 mm	diam
Target-beam collimator	0.1 rad	angular half-width of cone
State-Selector magnets		
Inner bead radius	4.7 mm	
Outer bead radius	5.6 mm	
Separation	3.9 mm	
Max. field, polarizer	11 KOe	Permanent magnet
Max. field, analyzer	21 KOe	Electro-magnet
Length of polarizer	12 cm	
Length of analyzer	15 cm	

oven with capacity for about 25 g of alkali metal. The vapor in the oven escapes through a column of five holes each 0.6 mm in diam which are spaced 2 mm apart along a vertical line. A hot skimmer mounted about 2 cm from the holes restricts the width of the beam to about 0.2 mm. This array is preferable to a single hole at low intensities (where the flow of atoms is effusive), because it produces a more uniform beam in the vertical direction. At high intensities (where the flow is supersonic) a cloud of atoms forms near the skimmer, limiting the intensity (measured after the skimmer) to roughly 10^{17} atom/sec sr. Scattering in this cloud produces a beam whose uniformity and intensity are quite independent of the details of the orifice array.

Two completely different sources were used at different times to produce the target beam; we describe here only the more successful one, a recirculating source which produces a beam directed vertically upward. It consists of a two-chamber oven with a single 0.8-mm-diam hole at the top of the upper chamber. The beam is defined by a 2.5-mm-diam aperture located 2.5 cm above the source. The vapor which does not pass through the beam-defining aperture condenses on the inside of a water-cooled jacket, where it may be melted and drained back into the lower chamber of the oven by passing steam through the water-cooling lines.

D. Detector

The detector is a surface ionizer followed by a mass spectrometer and a magnetic-strip electron multiplier. We have been able to reduce the noise level to as low as 1 ion/sec per mm^2 of detector area, an essential achievement in view of the large loss in counting rate due to the state-selection devices.

The dominant source of noise in the detector is alkali impurities in the filament. We use an iridium filament, [11] which we flash near the breaking point for about 1 h and then age for several days at the operating temperature – the minimum temperature (a dull red) commensurate with usefully short response time, typically 10 msec. Undisturbed aging at operating temperature seems to be a key factor in reducing the noise, and for this reason we place the detectors in a separate chamber which is constantly maintained under high vacuum. Since hydrocarbons appear to produce excess filament noise, the detector chamber is pumped with a VacIon pump.

E. Velocity Selector

The velocity selector is similar to conventional slotted-disk velocity selectors except that all of the disks are thin so that particles with several widely different velocities may pass simultaneously. [12] In practice, the narrow velocity distribution of our source, together with the rough velocity selection provided by the state-selector magnets, removes all ambiguity about which velocity passband is in use. Since the sidebands have different resolutions, this arrangement permits us to vary the resolution in the course of the experiment. [Data presented here were taken with velocity resolution R_v of 10% or 5% full width half-maximum (FWHM).] In addition, we can eliminate any uncertainty in absolute-velocity calibration due to misalignment of the selector by comparing velocity profiles taken with the selector rotating in opposite directions. [13]

F. Scattering Geometry

Figure 2 illustrates the two scattering geometries which have been used. In the first (which we designate by G1) the incident, scattered, and target beams were in the same plane. The target beam was produced in a conventional oven with a crinkled metal-foil collimator. We assume that the velocity distribution was Maxwellian.

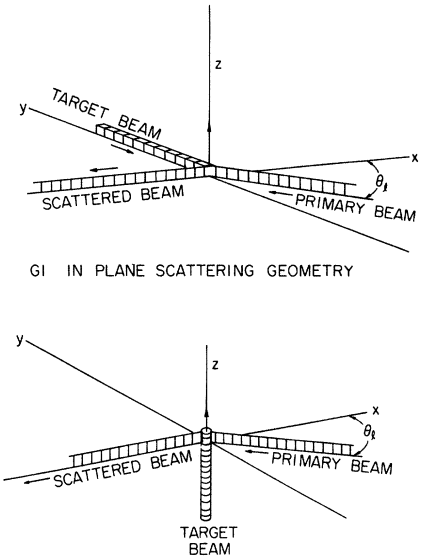

FIG. 2. Comparison of the two different scattering geometries used in the experiment.

The second geometry (G2) utilizes a target beam directed perpendicularly to the plane of the incident and scattered beams. This was introduced to permit the use of the recirculating jet source described above and to reduce the changes in relative velocity caused by the finite width of the target-beam velocity distribution. The velocity distribution and dimer concentration of this source were measured, and found to be 30% FWHM and ~2% respectively. We found that the most probable velocity was close to $(5kT/M)^{1/2}$, as expected for a jet source. This source produced data of higher quality than the first source because of the improved intensity and narrower velocity distribution.

III. MEASUREMENT PROCEDURE AND DATA ANALYSIS

In a typical single-channel scattering experiment (one with no state selection, e.g.) one measures the counting rate for atoms scattered through various angles. Assuming that noise has been eliminated by some combination of beam modulation and signal averaging, the counting rate must be multiplied by factors accounting for various characteristics of the apparatus in order to obtain the laboratory scattering cross section. Normally, factors accounting for beam intensities, scattering geometry, solid angles, detector sensitivity, etc. must be included to obtain the laboratory scattering cross section. (Only changes in these quantites are important if no attempt is made to determine the absolute differential cross section.) If the data are to be presented in the c.m. coordinate system then further corrections must be introduced.

In our experiment, the primary-beam atoms are prepared in a given state, and at each angle we measure two counting rates: N_{ex} (the detection rate for scattered atoms with changed state) and N_{nx} (the detection rate for atoms with no observable change of state). In order to present the related cross sections one must correct for apparatus effects to find the laboratory cross sections $\sigma'_{ex}(\theta_l)$ and $\sigma'_{nx}(\theta_l)$ and then transform the results to the c.m. system, just as in single-channel scattering. (The prime indicates quantities which have undergone corrections to the laboratory system.) Both types of corrections are complicated by the addition of the second channel: In addition to the apparatus effects mentioned above, one must correct for the imperfect performance of the state selectors; and in order to obtain the electron spin-exchange cross section, one must also correct for the complications of nuclear spin.

In this section we discuss the measurement procedure, our modulation- and signal-averaging techniques, the corrections for apparatus geometry and performance, and the corrections due to imperfections of the state selectors and to nuclear spin.

We generally express our measurements of σ'_{ex} and σ'_{nx} in terms of two new quantities, the "sum" cross section σ'_{sum} and the probability for change of state P'_{ex}:

$$\sigma'_{sum}(\theta_l) = \sigma'_{ex}(\theta_l) + \sigma'_{nx}(\theta_l),$$

$$P'_{ex}(\theta_l) = \sigma'_{ex}(\theta_l)/\sigma'_{sum}(\theta_l).$$

These variables simplify experimental analysis, since the apparatus effects generally affect one of these variables strongly and the other weakly, if at all. For example, variations in beam intensity, apparatus geometry, and other angle-dependent factors affect $\sigma'_{sum}(\theta_l)$, but not $P'_{ex}(\theta_l)$ (which contains the same correction factor in both numerator and denominator). Imperfect state-selector performance, on the other hand, affects P'_{ex} primarily, since $\sigma'_{sum}(\theta_l)$ is the sum of cross sections over final spin state. (If an atom goes the "wrong way" in a state selector, this does not affect the total number of atoms which emerge.)

A. Measurement Procedure

Each experimental run to determine P'_{ex} and σ'_{sum} consists of a series of measurements of N_{ex} and N_{nx} taken at different angles, but with the same final velocity. Occasionally, measurements of σ'_{sum} are made directly by turning off the analyzer magnet. Each measurement consists of 4–15 count periods, each generally about 5 sec long, during which the target beam is chopped at approximately 2 Hz, while the signal from the detector is gated synchronously between two scalar inputs. The mass spectrometer in the detector eliminates all

background from the target beam, so that the difference between readings of the two scalers is the desired signal. Problems in eliminating background from the target beam have so far prevented study of collisions between identical alkalis.

Although the apparatus was designed to use two detectors simultaneously, we have generally found that better results can be obtained by using only the quieter detector. Measurements of N_{ex} and N_{nx} are then made by changing the source polarization, while the rest of the apparatus is left undisturbed. In order to determine the asymmetry factors of the source and detector, it is necessary to measure N_{ex} and N_{nx} both by moving the detector and by changing the source polarization for at least one angle (this involves four distinct measurements).

Although the target-beam intensity is continuously monitored, the geometry of the experiment makes it impossible to monitor continuously the intensity of the primary beam in the scattering region. Fortunately, changes in primary-beam intensity are generally slow enough to be monitored by repeating measurements at some reference angle periodically throughout the run. This also reduces effects due to any slow changes in detector sensitivity.

In addition to the scattering data, a standard set of measurements is taken on the primary beam in order to determine the degree of its polarization for both possible source polarizations. These measurements are made by inserting the attenuator in the incident beam, setting the source carriage to zero angle, and using the velocity selector, analyzer magnet, and detector in the usual manner. This technique also permits us to select the oven positions which give the highest intensity at the desired velocity. In practice, we alter these selections slightly to achieve essentially identical velocity distributions for source beams of opposite polarization. The intensities of these two beams are noted for later use. (They are not quite equal due to the slight focusing and defocusing properties of the polarizing magnet.)

B. Statistical Errors

The large amount of data taken in our experiment is analyzed on a computer. This subsection describes the development and application of techniques designed to reduce the noise and estimate the reliability of the data.

Each measurement of N_{ex} or N_{nx} at a particular angle and velocity consists of 4–14 pairs of scalar readings; each pair consists of the total number of counts obtained with the target beam on, N^+, and with the target beam off, N^-, during one count period. (We suppress the subscripts in this section.) If the detector noise were purely stochastic, then the variance would be purely statistical: $\sqrt{N}$ where N is the mean number in a single counting period for a given channel. However, when we compute the variance we find that it generally exceeds the statistical variance. The excess noise comes from the detector filament which emits ions in clumps rather than at random. The intermittent nature of this noise makes it imperative to discard some of the data, but the non-random character of the filament noise prevents us from doing so with criteria based on the statistical noise only.

The most satisfactory rejection criterion which we found was based on the geometric mean of the observed variance and the statistical variance. We rejected points differing from the mean by approximately twice this amount. The mean and the variance were recomputed after each point was discarded, and this process was repeated until all remaining points were within the criterion, or until 50% of the data was discarded (this occurred only a few percent of the time). The statistical errors shown on the data points are the product of the observed variance and the ratio of the number of raw-data points to the number of points retained.

This criterion is applied separately to the measurements of N^+, N^-, and to $N_{sig}=N^+-N^-$. The average signal $\langle N_{sig}\rangle$ is then determined in two ways:

$$\langle N_{sig}\rangle_1=\langle N^+\rangle-\langle N^-\rangle, \qquad \langle N_{sig}\rangle_2=\langle N_{sig}\rangle.$$

Since the rejection criteria are applied independently in each averaging process, $\langle N_{sig}\rangle_1$ and $\langle N_{sig}\rangle_2$ do not necessarily agree. The difference, if any, is treated as an independent error in calculating our final error. All errors reported in this paper are about 70% confidence limits, and represent purely statistical errors. Possible systematic errors are discussed separately.

C. Corrections Affecting σ'_{sum}

In order to determine cross sections from the counting rates, it is necessary to determine the effective size of the scattering volume, the relative velocity, and the beam intensities. Although we have not attempted to make accurate absolute determinations of the cross sections, we have taken care to determine precisely their angular dependence.

The effective size of the scattering volume depends on the scattering angle in a complicated fashion; necessary corrections for this are made numerically. Both the relative velocity in the c.m. system and the initial primary-beam velocity change with angle because the velocity analyzer is in the scattered beam. For the same reason, the range of incident-beam velocity which can contribute to observable scattering events changes slightly with angle, causing a spurious angle-dependent factor in the cross section. However, the corrections for these effects are very small and are made easi-

ly. We neglect a still smaller correction due to change in intensity of the incident beam with incident velocity, since its velocity distribution is constrained to be essentially flat over the range involved by our selection of the oven positions.

Uncertainties in the above corrections are the dominant sources of systematic error in the sum cross section. In particular, nonuniformity of the target beam, especially when it is accentuated by target-beam misalignment, can cause errors in the calculation of the scattering volume. We estimate that this effect could smoothly decrease σ_{sum} by as much as 10% for angles less than 200 mrad.

Undetected fluctuations in the intensities of the colliding beams is the second major source of error. We believe that this introduces an uncertainty of less than 3% in adjacent points and less than 15% for any two points in a given set of data. Since the amplitude of the structure observed in the experiment is considerably larger than these limits, the undetected intensity fluctuations are not a serious source of error in resolving angular structure or in determining the location of the maxima and minima observed.

D. Corrections Affecting Probability of Exchange

P'_{ex} is not affected by the processes described in the preceding subsection: σ'_{ex} and σ'_{nx} are corrected by the same factor (unless the beam intensities are changing rapidly), which leaves their ratio unchanged. However, a different set of errors affects P'_{ex}. These are of two types, both stemming from imperfect performance of the state-selection magnets. The first results from a difference in solid angle for atoms with opposite polarization, which is due to the slight focusing properties of the dipole-field deflection magnets. This is manifest as a difference in the detector solid angle for oppositely polarized atoms (we call this detector asymmetry) or as a polarization-dependent intensity in the primary beam. These effects are readily corrected by comparing measurements of σ'_{ex} and σ'_{nx} made with opposite source polarizations. Their effect on P'_{ex} is primarily multiplicative, and the correction is generally less than 15% of P'_{ex}. Uncertainty in the asymmetries causes an error in P'_{ex} of 10% of its value. Since this is essentially a multiplicative error, we do not include it in the error bars in Figs. 8–12, because it has the same effect on all points in each run and therefore does not detract from our ability to resolve angular structure in the probability of exchange.

The second state-selector imperfection is incomplete separation of the two polarization states due to inadequate deflection power and small angle scattering from gas in the beam collimators. This appears to be a problem only with the source. It results in incomplete polarization of the primary beam, or, in more graphic terms, in source-beam impurity. We correct for this by measuring the impurity in the primary beam as outlined earlier, and correcting the data for P'_{ex} accordingly. The correction is principally subtractive. We believe, however, that this correction is reliable only when the impurity fraction α, is less than 0.02. This judgement is based on a comparison of the values obtained when $P'_{ex}(\theta)$ is extrapolated to zero angle. For all measurements (about half) with impurity less than 2%, this extrapolation yields 0 within error, which is in accord with theoretical prediction; while for all measurements made with impurity greater than 2%, the extrapolated value of $P'_{ex}(0)$ is greater than 0. We believe that this unreliability of the impurity correction stems from the fact that the detector solid angle is not large enough to encompass the entire source beam, so that the top, bottom, or sides of the beam might have higher impurity fraction than the part measured.

In those runs with beam impurity greater than 2%, we have treated α as an adjustable parameter, choosing its value so that P_{ex} approached 0 for small angles. The value of α used in these runs is indicated as α_c in Figs. 8–12.

Because we are unable to correct adequately for the beam impurity when it exceeds 2%, the value of our results at small angles (where P'_{ex} is small) is decreased when the beam impurity factor α exceeds 0.02. However, this does not change the location of the oscillatory maxima and minima in P'_{ex}, and it does not hinder us in observing the structure in P'_{ex} since the impurity is the same for all angles.

E. Corrections for Nuclear Spin

The measured cross section for change of state, σ'_{ex}, and the measured probability of change of state, P'_{ex}, are not equal to the corresponding cross section and probability for electron spin exchange. This is due to the coupling between the electron spin and the nuclear spin of the primary atom. In this section, we describe how we find the cross section for electron exchange, σ_{ex}, and the probability of electron exchange, P_{ex}, from our measurements of σ'_{ex} and P'_{ex}.

Our state selectors operate at a high magnetic field which decouples the nuclear and electron spins, selecting atoms on the basis of electron spin projection alone. The collision occurs in a region of low magnetic field (about 8 Oe), however, where good quantum numbers for the primary atom are F and m_F, the total spin and its projection on the Z axis, respectively. (Care was taken to assure that the atoms change adiabatically from the high field in the state selector to the low field in the scattering region.) Thus, we need to consider the relationship between exchange of electron spin during the collision and observable changes of hyperfine state

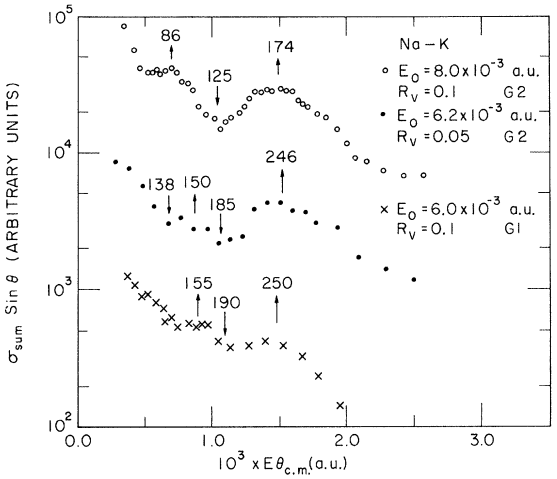

FIG. 3. σ_{sum} versus $E\theta$ for Na-K. The number above each maximum or minimum in $\sigma_{sum}(E\theta)$ is the c.m. angle of the feature (in mrad). R_v is the velocity selector resolution.

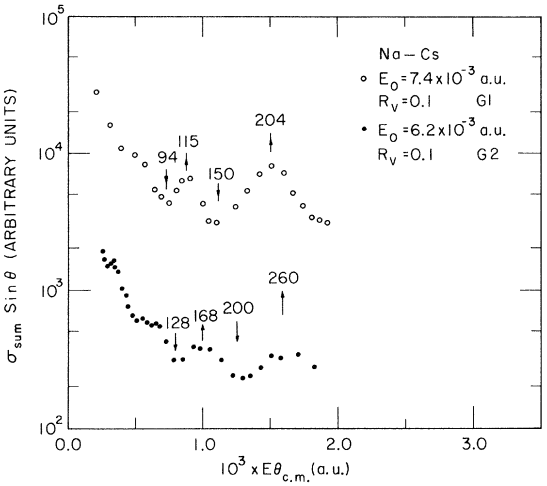

FIG. 5. σ_{sum} versus $E\theta$ for Na-Cs.

(i.e., those which connect adiabatically to high-field states having opposite electron spin projection).

If there is no electron spin exchange in the collision, then the atom's hyperfine state is not changed, and its high-field electron polarization is not reversed. If there *is* electron spin exchange, then it is possible that the new hyperfine state may have the same high-field electron spin as the original state. Thus, the only possible effect of the nuclear spin is to prevent an electron spin-exchange collision from being observed. Burnham's exact results[14] show that

$$P_{ex} = P'_{ex}/m(I),$$

where P_{ex} is the probability of electron spin exchange and

$$m(I) = (4I^2 + 2I + 1)/(4I^2 + 4I + 1).$$

This expression shows that $m(I)$ lies between 0.75 ($I = \frac{1}{2}$) and 1.0 ($I = 0$ and $I \to \infty$). [Both Na and K have nuclear spin $\frac{3}{2}$, $m(\frac{3}{2}) = 0.813$.] We also have

$$\sigma_{ex} = \sigma'_{ex}/m(I).$$

The nuclear spin has no effect on the total number of atoms scattered in a particular direction, so σ'_{sum} requires no correction for nuclear spin.

The above results apply to collisions occurring at low magnetic field, and P_{ex} is defined to be the probability of electron spin exchange for collisions with unpolarized targets. The behavior of exchange cross sections for polarized targets (including effects of magnetic field and nuclear spin) is more complicated and will be discussed elsewhere.[15]

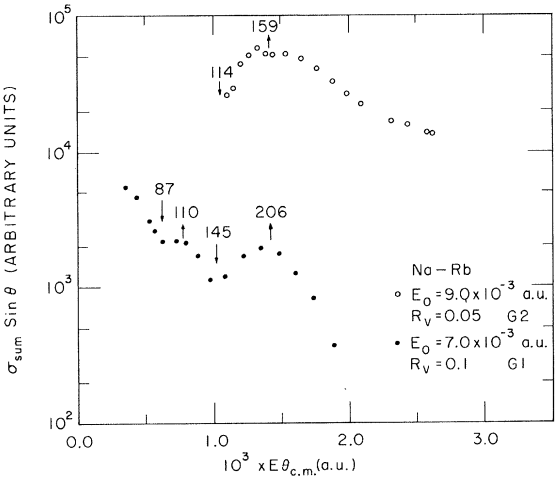

FIG. 4. σ_{sum} versus $E\theta$ for Na-Rb.

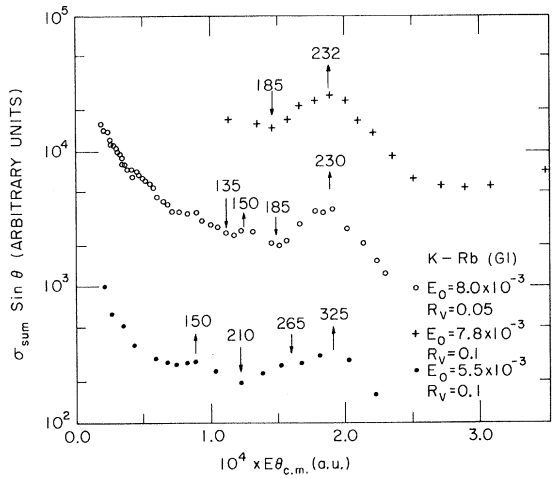

FIG. 6. σ_{sum} versus $E\theta$ for K-Rb.

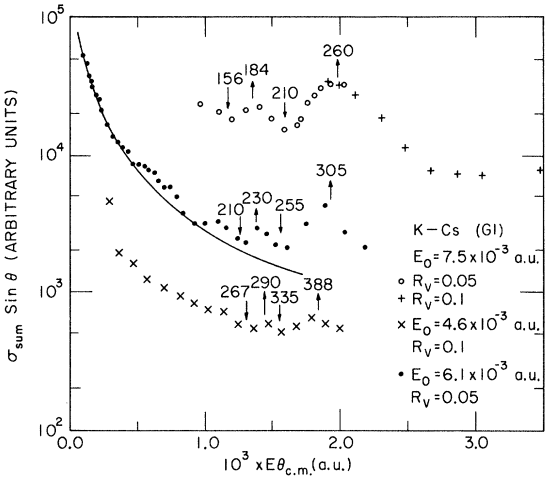

FIG. 7. σ_{sum} versus $E\theta$ for K-Cs. The solid line is a fit to the small-angle data based on $\sin(\theta)\sigma(\theta) \propto \theta^{4/3}$, the law expected from a $1/R^6$ potential.

F. Transformation to Center of Mass

At first it may appear that the transformation of the data to the c.m. coordinate system is complicated owing to the location of the velocity selector in the scattered beam. This is not the case, however, for the elastic scattering under study here. Since the kinetic energies studied ($\lesssim 10^{-2}$ a.u.) are far less than the lowest excitation energy for states of the separated atoms (~ 0.1 a.u. for the excitation of alkali valence electron to the adjacent p state), no inelastic processes are possible, and the initial c.m. velocity of the particles is uniquely determined from the final velocity (which is controlled by the velocity selector) and the initial velocity of the target beam (which is known – see Sec. II F). [However, the energy still changes slightly with angle. (The effects of this drawback of our geometry will be discussed in Sec. IV.)] Hence, the transformation from the laboratory coordinate system to the c.m. coordinate system depends entirely on kinematical considerations, and is relatively straightforward. In addition to changing the angle, this transformation also entails multiplication of the cross sections by the appropriate Jacobian. This angle-dependent factor changes σ_{sum} but not P_{ex}.

The velocity of the target beam does not enter critically into the transformation to c.m. coordinates, and we do not believe that the experimental uncertainties in target-beam velocity add significant uncertainty to the transformation. However, the internal motion of the target beam (which we assumed to be monoenergetic and perfectly collimated when making the transformation) increases the effective experimental resolution somewhat. This

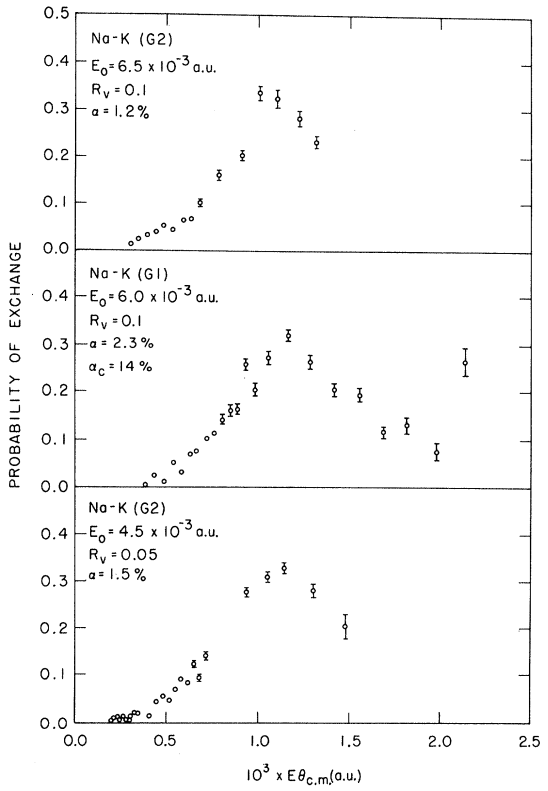

FIG. 8. P_{ex} versus $E\theta$ for Na-K.

change in v_{rel} is partially offset by a change in $\theta_{c.m.}$ such that the resolution in $E\theta$ is not degraded as much as the resolution in relative velocity. (We use the variable $E\theta$ as an independent variable in presenting our results.) We estimate that our ef-

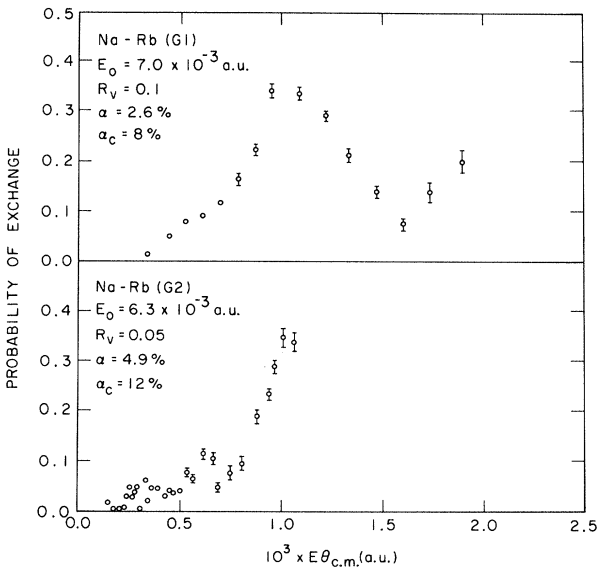

FIG. 9. P_{ex} versus $E\theta$ for Na-Rb.

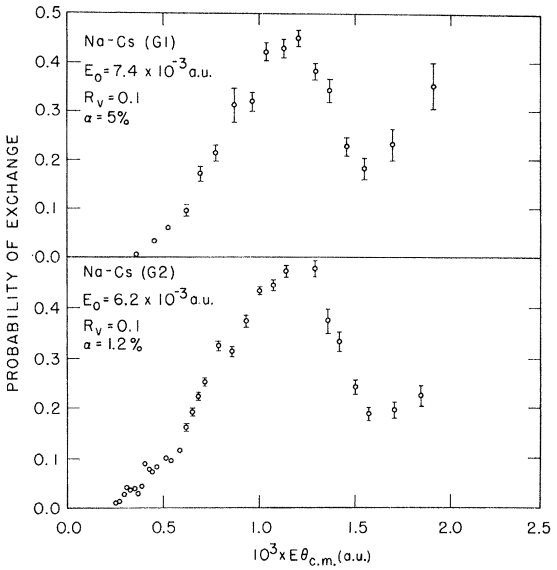

FIG. 10. P_{ex} versus $E\theta$ for Na-Cs.

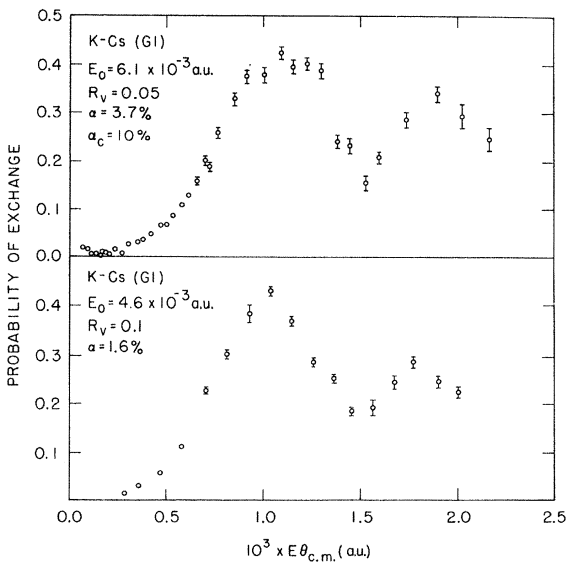

FIG. 12. P_{ex} versus $E\theta$ for K-Cs.

fective resolution in $E\theta$ is typically 14% (22%) for $R_v = 0.05$ (0.10). (The angular resolution of our apparatus is good enough so that it does not increase our effective resolution of $E\theta$.)

IV. RESULTS

We present here results for five different alkali-alkali systems; in three of these the primary beam is sodium (Na-K, Na-Rb, and Na-Cs), and in the other two the primary beam is potassium (K-Rb and K-Cs). This pairing assures that the target-beam atoms are heavier and cooler than the primary-beam atoms, which reduces undesirable averaging of the cross sections over poorly determined

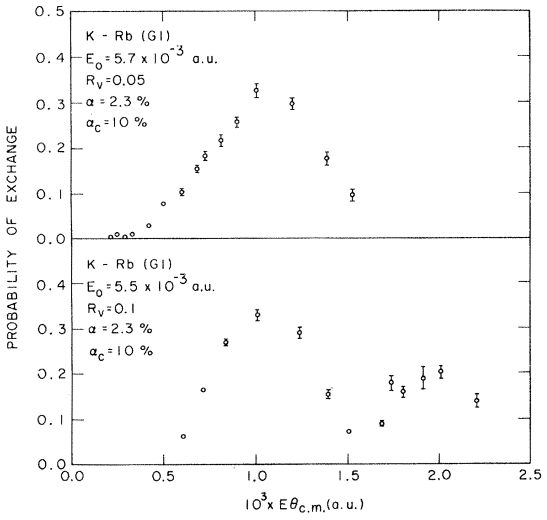

FIG. 11. P_{ex} versus $E\theta$ for K-Rb.

c.m. variables.

For each system studied, we present data taken at two or more different laboratory velocities. Since our velocity selector is in the scattered beam, the relative velocity of the incident atoms and the target atoms depends on the angle. This means that the c.m. energy increases slightly with angle (3% at the rainbow angle in K-Cs for $E_0 = 4.6\times10^{-3}$ a.u., the worst case encountered). The energy indicated for the data points is the c.m. energy at zero angle (where incident and final velocities are equal); it is labeled E_0 to emphasize this fact. Using the reduced variable $E\theta$ lessens the effects of the slight variation in energy.

We have made two checks of our results against work in other laboratories. Our results for $\sigma_{ex}(\theta)$ in K-Cs have been compared with those of Beck *et al.*,[7] and good agreement was found for both the general shape and the location of the maxima and minima. [The comparisons were made on an $E\theta$ plot; their results (for $E = 5.3\pm1.3\times10^{-3}$ a.u.) lie midway between ours at $E = 4.9\times10^{-3}$ and 6.1×10^{-3}]. As another check, we measured the rainbow structure in the system K-Xe (the Xe was introduced through a glass capillary array at 77 °K using geometry G2). When analyzed by the method described in Sec. V of the Paper II, this data yielded a well depth of $0.47\pm0.02\times10^{-3}$ a.u. ($2.02\pm0.07\times10^{-14}$ erg), in good agreement with the results of Buck and Pauly.[16] We used a Lennard-Jones 8-6 potential).

We have used the reduced angle $\tau = E\theta$ as the abscissa in Figs. 3–12. In the first-order impact approximation[17] collisions with the same impact parameter scatter to the same τ because τ is a

measure of the integral of the force of the interaction along the trajectory, and does not depend on the duration of the collision if the trajectory is nearly straight. The utility of this variable is apparent from examination of σ_{sum} in Figs. 3–7, for in each system the distinctive rainbow maxima[18] lie at nearly the same value of $E\theta$. (This is confirmation of the applicability of the impact approximation to these collisions.) It is apparent that the rainbow maxima of different systems all lie fairly close to $E\theta = 1.7\times10^{-3}$ a.u., although the rainbows for systems with Na as one component all lie below this value, while those for systems composed of heavier alkalis lie consistently above this value. (See Figs. 3–7.)

The curves for P_{ex} in Figs. 8–12 for the systems studied are quite similar. All curves start from 0 at small angles (although in some cases this results from our choice of α_c, see Sec. III D) and all have a large maximum where $P_{ex}\sim 0.4$ near $\tau = 1.0\times10^{-3}$ a.u. Further oscillations are evident in those cases where the data extends past this first maximum.

We analyze this data in a Paper II which follows.

ACKNOWLEDGMENTS

We would like to thank David C. Burnham for help in the design and construction of the apparatus, and Edward M. Mattison for a critical reading of the manuscript.

---

*Work supported by the Joint Service Electronic Program [Contract No. Da28-043-AMC-02536(E)] and by the NSF Grant No. GP-13633.

†Present Address: Science Department, U. S. Naval Academy, Annapolis, Maryland.

[1]U. Buck, and H. Pauly, Z. Physik 208, 390 (1968).

[2]E. M. Purcell and G. B. Field, Astrophys. J. 124, 542 (1956).

[3]J. P. Wittke and R. H. Dicke, Phys. Rev. 103, 620 (1956).

[4]H. G. Dehmelt, Phys. Rev. 109, 381 (1958).

[5]N. W. Ressler, R. H. Sands, and T. E. Stark, Phys. Rev. 184, 102 (1969).

[6](a) D. Pritchard, D. Burnham, D. Kleppner, Phys. Rev. Letters 19, 1363 (1967); (b) *Abstracts, International Conference on Atomic Physics*, 1968 (New York U. P., New York, 1968, p. 147; (c) *Abstracts, Sixth International Conference on the Physics of Atomic and Electronic Collisions, July* 1969, (M. I. T. Press, Cambridge, Mass., 1969), p. 31.

[7]D. Beck, U. Henkel, A. Schultz, Phys. Letters 27A, 277 (1968).

[8](a) R. E. Collins, B. Bederson, M. Goldstein, and K. Rubin, Phys. Letters 27A, 440 1968; (b) Phys. Rev. Letters 19, 1366 (1967); (c) Ref. 6(b), p. 117; (d) Ref. 6(c), p. 781.

[9]Apparatus: D. E. Pritchard, D. C. Burnham, G. M. Carter, and D. Kleppner, Ref. 6(c), p. 37.

[10]N. F. Ramsey, *Molecular Beams*, (Oxford U. P., Oxford, England,1956).

[11]Obtained from Sigmund Cohn Co., Mt. Vernon, N.Y.

[12]See J. R. Kinsey, Rev. Sci. Instr. 37, 61 (1966) for references.

[13]A. E. Grosser [A. E. Grosser, Rev. Sci. Instr. 38, 257 (1967)] made a selector with different resolution for clockwise and counterclockwise rotation, permitting the elimination of this source of error.

[14]D. C. Burnham, Ph. D. thesis, Harvard University, 1966 (unpublished); and Phys. Rev. 185, 399 (1969). See also Paper II, Eqs. (3) and (4).

[15]G. M. Carter and D. E. Pritchard (to be published).

[16]U. Buck and H. Pauly, Z. Physik 208, 390 (1968).

[17]F. T. Smith, R. P. Marchi, and K. G. Diedrick, Phys. Rev. 150, 79 (1966).

[18]Rainbow Scattering: See K. W. Ford and J. A. Wheeler, Ann. Phys. (N. Y.) 7, 259 (1959); or a modern review such as H. Pauly and J. P. Toennies, Advan. At. Mol. Phys. 1, 195 (1965).